JCI insight

Lung group 2 innate lymphoid cells are trained by endogenous IL-33 in the neonatal period

Catherine A. Steer, … , Hanjoo Shim, Fumio Takei

JCI Insight. 2020. https://doi.org/10.1172/jci.insight.135961.

Research In-Press Preview Immunology

Graphical abstract

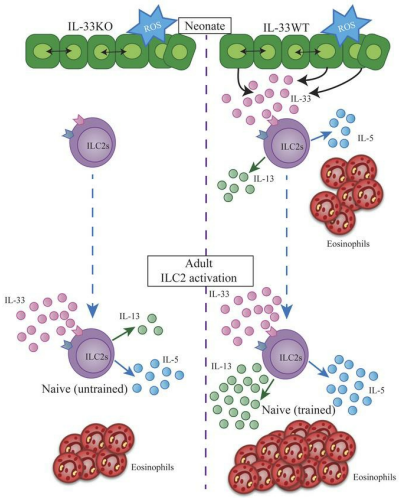

Lung group 2 innate lymphoid cells are trained by endogenous IL-33 in the neonatal period

Catherine A. Steer, PhD.[1*], Laura Mathä, B.Sc.[1,2], Hanjoo Shim, B.Sc[1**], Fumio Takei, PhD.[1,3†]

Affiliations: [1]Terry Fox Laboratory, British Columbia Cancer Agency, Vancouver, B.C., Canada. [2]Interdisciplinary Oncology Program, University of British Columbia, Vancouver, B.C., Canada. [3]Department of Pathology and Laboratory Medicine, University of British Columbia, Vancouver, B.C., Canada.

[*]Current address: Department of Laboratory Medicine, University of California, San Francisco, San Francisco, CA, U.S.A.

**Current address: Department of Microbiology, Immunology and Infectious Diseases, University of Calgary, Calgary, AB, Canada.

[†]**Corresponding author:** Fumio Takei

ftakei@bccrc.ca

604-675-8131

675 West 10th Ave., Vancouver, BC, V5Z IL3

Conflict of interest:

The authors declare no conflict of interest.

Abstract:

Group 2 innate lymphoid cells (ILC2s) in mouse lungs are activated by the epithelium-derived alarmin IL-33. Activated ILC2s proliferate and produce IL-5 and IL-13 that drive allergic responses. In neonatal lungs, spontaneous activation of lung ILC2s occurs dependent on endogenous IL-33. Here we report that neonatal lung ILC2 activation by endogenous IL-33 has significant effects on ILC2 functions in adulthood. Most neonatal lung ILC2s incorporated 5-bromo-2'-deoxyuridine (BrdU) and persisted into adulthood. $BrdU^+$ ILC2s in adult lungs responded more intensely to IL-33 treatment than $BrdU^-$ ILC2s. In IL-33 deficient (KO) mice, lung ILC2s develop normally but they are not activated in the neonatal period. Lung ILC2s in KO mice responded less intensely to IL-33 in adulthood compared to wild type (WT) ILC2s. While there was no difference in the number of lung ILC2s, there were fewer $IL\text{-}13^+$ ILC2s in KO than WT mice. The impaired responsiveness of ILC2s in KO mice was reversed by intranasal administrations of IL-33 in the neonatal period. These results suggest that activation of lung ILC2s by endogenous IL-33 in the neonatal period may "train" ILC2s seeding the lung after birth to become long-lasting resident cells that respond more efficiently to challenges later in life.

Introduction

Group 2 innate lymphoid cells (ILC2s) are key drivers of type 2 immunity (1). Lung ILC2s respond to the alarmin IL-33 released by epithelial cells upon exposure to inhaled allergens and secrete large amounts of IL-5 and IL-13. IL-5 promotes eosinophil differentiation, recruitment, activation, and survival. IL-13 is responsible for goblet cell hyperplasia, mucus secretion, collagen secretion from fibroblasts, and drives development of alternatively activated macrophages (2). Additionally, IL-13 promotes T helper 2 (TH2) cell differentiation (3-6). Through the production of those type 2 cytokines, lung ILC2s play a key role in allergic lung diseases, tissue repair, lung fibrosis, and anti-parasite immunity (7, 8).

Analyses of parabiosis mice showed that ILCs are tissue resident lymphocytes and very few ILCs circulate in adult mice (9). Recently, Schneider et al. have also shown that most ILC2s in adult mouse lungs develop in the neonatal period, and only a minor fraction is slowly replaced by newly developing ILC2s in adulthood (10). Therefore, the neonatal period is critical for ILC2 development. We (11) and others (12-14) have found that lung epithelial and stromal cells express IL-33 around 10 to 14 days after birth. This may be due to early life signals including the mechanical stretch of the first few breathes of life, oxidative stress, or even lung developmental processes. The wave of IL-33 causes transient activation and proliferation of neonatal lung ILC2s and eosinophil infiltration. It is thought that the activation of ILC2s is responsible for the TH2 biased response to antigens in the neonatal period (11).

We have previously shown that activation of adult mouse lung ILC2s by inhaled allergen or recombinant IL-33 have long lasting effects on ILC2 functions (15). After the resolution of

inflammation, some activated ILC2s persist for several months as resting “allergen experienced” memory cells that are more responsive to inhaled allergens or IL-33 than naïve ILC2s. Upon challenge with an unrelated allergen or IL-33, months after the first allergen exposure, memory ILC2s vigorously respond and induce enhanced airway inflammation characterized by increased numbers of eosinophils in the lung and higher mucus accumulation in the airways compared with naïve mice receiving the same challenge.

While the exact mechanism behind ILC2 memory has yet to be elucidated, our transcriptome analyses of purified naïve and memory ILC2s identified a small set of differentially expressed genes that included *Il17rb* encoding the IL-25 receptor (15). The expression of *Il17rb* was very low in naïve lung ILC2s but was rapidly upregulated by activation and the higher expression of *Il17rb* was maintained in memory ILC2s for more than 4 months after the initial activation. Flow cytometric analyses confirmed higher expression of the IL-25R on memory compared to naïve lung ILC2s. Furthermore, memory, but not naïve, lung ILC2s were activated by intranasal administration of IL-25. These results suggested that IL-25R upregulation is an ILC2-intrinsic mechanism by which lung ILC2s acquire memory functions.

We now have investigated whether the activation of neonatal lung ILC2s by endogenous IL-33 has a similar effect as adult ILC2 activation which results in the generation of memory ILC2s. ILC2s in IL-33 deficient (KO) mice are not activated in the neonatal period (11). Therefore, we compared lung ILC2s from KO and wild type (WT) mice. Our results show that activation of lung ILC2s in the neonatal period makes them more functionally competent in adulthood. This process is different from the generation of memory ILC2s in adult mice. The former does not involve

acquisition of new functions whereas memory ILC2s become responsive to IL-25 (15). Therefore, we termed the process “ILC2 training.”

Results

Characterization of neonatal lung ILC2s. We previously found that the ILC2 population in the lung expands around 10 days after birth, and this was not observed in other tissues (11). Immunohistochemical analysis of neonatal lung suggested that endogenous IL-33 is elevated at the time of ILC2 expansion (11). To further investigate the activation of neonatal lung ILC2s, we first analyzed the amounts of IL-33 in neonatal mouse lung homogenates. Enzyme-linked immunosorbent assay (ELISA) analysis of lung homogenates showed that the amounts of IL-33 were elevated around 10 days after birth (Figure 1A). Lung ILC2s in this period highly expressed the proliferation marker Ki-67 (Figure 1B). Neonatal ILC2s expressed the IL-25R (Figure 1C) and responded to intranasal administration of IL-25 (Figure 1D). In contrast, naïve adult lung ILC2s expressed very low amounts of IL-25R and did not respond to intranasal IL-25. The protease allergen papain, along with other allergens, induces IL-33 mediated allergic inflammation but also induces the release of IL-25 (16). As expected, exposure to papain in the neonatal period led to more ILC2 proliferation and intracellular IL-5 and IL-13 expression compared to those treated in adulthood (Figure 1E,F).

We then compared the global gene expression profile of neonatal lung ILC2s with those of naïve adult lung ILC2s and after activation by recombinant IL-33 (effector adult) (Figure 1G). As expected, based on the protein expression, neonatal lung ILC2s had a higher expression of *Mki67*, *Il5* and *Il13* compared to naïve adult ILC2s. Neonatal lung ILC2s also had a higher expression of

activation-associated genes than naïve adult ILC2s, including the gene encoding the decoy IL-1 receptor *Il1r2* (15, 17), and ILC2-activation associated micro-RNA *Mir155* (18, 19). However, neonatal ILC2s differed from effector adult ILC2s in the expression of several genes. The former had a slightly lower expression of *Il1r2* (Supplemental Figure 2A), as well as *Tnfrsf8* and *Anxa2*, genes that have been previously shown to be overexpressed in asthmatics (Figure 1G) (20-22). Neonatal and naïve adult ILC2s had a higher expression of *Cd24a* than effector adult ILC2s, which was confirmed by flow cytometry (Figure 1G, Supplemental Figure 2B). Effector adult ILC2s also had higher expression of the checkpoint molecule genes *Pdcd1* and *Ctla4,* which are upregulated in activated ILC2s (23, 24), although protein expression of intracellular CTLA4 was not different between neonatal and adult effector ILC2s (Supplemental Figure 2C). Effector ILC2s expressed lower levels of *Nmur1* than naïve adult and neonatal ILC2s. *Nmur1,* which encodes neuromedin-U receptor 1, has been known to be downregulated in response to IL-33 treatment (25) (Figure 1G, Supplemental Figure 2D). Neonatal ILC2s also had a higher expression of *Vegfa*, encoding vascular endothelial growth factor A, than adult naïve and effector ILC2s suggesting a role in lung development as has been proposed previously (12). However, this was not recapitulated with qPCR analysis (Supplemental Figure 2E). Additionally, periodic acid-Schiff staining (PAS) of 10 days old mouse lungs confirms that the amount of cytokine being released by activated neonatal ILC2s is not sufficient to induce mucus secretion, a hallmark of type 2 inflammation (data not shown).

Gene set enrichment analysis (GSEA) showed that the differences in gene expression between naïve adult and neonatal lung ILC2s were very similar to those between naïve and activated $CD4^+$ T cells (Figure 1H) whereas the differences between neonatal ILC2s and effector adult lung ILC2s were similar to those between memory and effector $CD8^+$ T cells (Figure 1I). These results

suggested that activation of neonatal lung ILC2s by endogenous IL-33 is not as strong as activation of adult ILC2s by exogenous recombinant IL-33.

Neonatal lung ILC2s persist and respond more vigorously than those that develop in adulthood. Intranasal (I.N) 5-bromo-2'-deoxyuridine (BrdU) administration from postnatal day 6 to 9 resulted in 77% of lung ILC2s labelled with BrdU at postnatal day 10 (Figure 2A). Two weeks and 49 days after the BrdU treatment, 67% and 32% of the adult ILC2 population, respectively, was $BrdU^+$, indicating that neonatal ILC2s persisted into adulthood, as previously reported (11, 26). ILC2s are tissue-resident at steady state (9), and it is unlikely that the decrease in the BrdU-labelled ILC2s was due to their migration out of the lung. Adult mice given BrdU in their drinking water for 6 weeks had ~26% of their ILC2s labelled with BrdU, indicating a very slow turnover of lung ILC2s in adulthood (Figure 2B). These findings are consistent with the recent report showing that most adult mouse ILC2s develop in the neonatal period and they are very slowly replaced by newly developing ILC2s in adulthood (10).

We next investigated if there is a difference in responsiveness of neonatal ($BrdU^+$) ILC2s versus $BrdU^-$ ILC2s in the adult period. Two I.N injections of IL-33 (0.5 μg) were given to adult mice which had been given I.N BrdU in the neonatal period (Figure 2C). $BrdU^+$ ILC2s (red) more intensely expressed intracellular IL-13 compared to the $BrdU^-$ (black) ILC2s (Figure 2D, right plot). A higher proportion of $BrdU^+$ ILC2s were positive for IL-13 (Figure 2E). Therefore, neonatal ILC2s that persist in adult lungs are more responsive to IL-33 stimulation than ILC2s that develop in adulthood.

ILC2s from IL-33 deficient adult mice respond to IL-33 treatment more weakly than wild type mouse ILC2s. To test the effects of neonatal exposure to endogenous IL-33 on ILC2 functions in adulthood, we compared lung ILC2s from adult wild type (WT) and IL-33 deficient (KO) mice. KO mice are not exposed to endogenous IL-33 and not activated in the neonatal period (11). We gave two daily I.N administrations of IL-33 (0.5 μg) into KO and WT littermates at 8 weeks of age and analyzed the lung three days later (Figure 3A). IL-33 deficiency had no significant effect on the number of lung ILC2s in adulthood at steady state and after IL-33 treatment, they equally expanded (Figure 3B). However, intracellular cytokine staining showed the intensity of IL-13 and IL-5 was significantly less in lung ILC2s from KO mice than WT mice (Figure 3C and D). Interestingly, the numbers of IL-13$^+$ ILC2s from KO mice were significantly less than those from WT mice, while there was no significant difference in the number of intracellular IL-5$^+$ ILC2s (Figure 3E). Nevertheless, eosinophil numbers in KO mouse lungs were lower than in WT lungs (Figure 3F). Analysis of bronchoalveolar lavage also showed less IL-13, but not IL-5, in KO than WT mice (Figure 3G). I.N IL-33 induced less mucus production in KO than WT mouse lungs (Figure 3H). These results suggest that lung ILC2s in KO mice respond more weakly than WT to I.N IL-33 administration in adulthood.

Gene expression analysis demonstrates intrinsic differences between KO and WT ILC2s. We compared the gene expression profiles of lung ILC2s from adult KO and WT mice. There was no difference in the expression of *Il13, Il5, Gata3* and *Rora* (Figure 4A). WT ILC2s had a higher expression of the proinflammatory gene *Tnf*, the anti-apoptotic related gene *Bcl2a1d, Tnfsf10* encoding the TNF-related apoptosis-inducing ligand (TRAIL)*, Ltb4r1* encoding the activating receptor of leukotriene B4, and *Hdac3* encoding the histone deacetylase. KO ILC2s have a higher

expression of *Icam4, Icos, Cd24a*, and *Cdh5*, genes associated with cell adhesion and activation, and *Dusp10*, a regulatory enzyme (27). We confirmed protein expression of CD24, ICOS and intracellular TNF (Figure 4B). It should also be noted that WT ILC2s had a lower protein expression of ST2 than KO ILC2s, likely due to ligand-induced internalization (28), reflecting an environment of constitutive expression of IL-33 in adulthood in WT mice, albeit at low levels (Figure 4C, Figure 1A). These results highlight intrinsic differences between WT and KO ILC2s.

Neonatal IL-33 administration into KO mice reverses impaired ILC2 functions in adulthood.

To test if the weak responsiveness of KO ILC2s (shown in Figure 3) was due to the lack of activation in the neonatal period, we investigated if administrations of recombinant IL-33 into KO neonates were able to rescue the weak responses to IL-33 later in life. In this experiment, IL-33 was administered only once in adulthood (Figure 5A). This weakly activated ILC2s and highlighted the differences between WT and KO adult ILC2 responses. While there is slightly more ILC2s in WT mice than KO mice, the difference was not statistically significant (Figure 5B, left plot). As in Figure 3, WT mice had significantly more eosinophil recruitment than KO mice (Figure 5B, right plot), and higher frequency of IL-13^+ ILC2s (Figure 5C), but no difference in IL-5^+ ILC2s (Figure 5D). The frequency of IL-13^+IL-5^+ ILC2s is also higher in WT mice compared to KO mice (Figure 5E).

To rescue the KO response to a single IL-33 treatment, three daily I.N administrations of recombinant IL-33 (0.1 µg) into KO pups at 9 to 11 days after birth were given and six weeks later all groups were challenged with IL-33 (Figure 5F). Mouse lungs were analyzed for ILC2 proliferation, eosinophil recruitment and intracellular cytokine expression of ILC2s. Neonatal IL-

33 treatment significantly enhanced ILC2 proliferation beyond WT ILC2 numbers and increased eosinophil recruitment to the level of WT mice (Figure 5G). There were no differences in the frequencies of IL-5 IL-13 double positive ILC2s between WT and neonatally IL-33 treated KO mouse lungs (Figure 5H). The frequency of IL-13$^+$ ILC2s increased with neonatal IL-33 treatment in the KO mice in comparison to KO mice with no neonatal treatment, and there was no significant difference compared to the WT mice (Figure 5I). There was no difference between the groups in terms of IL-5$^+$ ILC2 frequency as expected (data not shown). These results suggest that the impaired responsiveness of lung ILC2s in adult KO mice is due to the lack of IL-33 in the neonatal period and can be rescued by neonatal IL-33 administration.

Discussion

ILC2s are tissue resident lymphocytes that develop early and persist throughout life (9, 10). We have previously shown that there are very few lymphocytes in newborn mouse lungs (11). While T, B and NK cell numbers steadily increase over 3 weeks to reach the adult levels, ILC2 numbers increase more rapidly, reaching the adult level (about $4x10^3$ cells per lung) by postnatal day 8 and then further increasing by four fold (to about $1.5x10^4$ cells per lung) between 10 and 14 days old. Previous studies have suggested that the expansion of the ILC2 population is due to IL-33 derived from lung epithelial and stromal cells (13, 14). Our current study has confirmed that the amount of IL-33 in the lung peak in 10 day old pups. Day 10 neonatal lung ILC2s express activation-associated genes and proteins, similar to adult lung ILC2s after I.N administration of recombinant IL-33. We then investigated the effects of the activation of neonatal lung ILC2s by endogenous IL-33 on adult lung ILC2s in two ways. First, we labelled neonatal ILC2s by BrdU and compared BrdU$^+$ and BrdU$^-$ ILC2s in adult lungs. The former were

activated in the neonatal period and persisted in adults whereas the latter were likely a mixture of neonatal ILC2s that were not activated by endogenous IL-33 and did not proliferate in the neonatal period (~25%, Figure 2A), those that lost BrdU due to cell proliferation, and ILC2s that newly developed in the adult period (~26% in 6 weeks, Figure 2B). $BrdU^+$ ILC2s in adult lungs responded more than $BrdU^-$ ILC2s to I.N administration of recombinant IL-33. We also compared lung ILC2s in adult WT and IL-33 KO mice. ILC2s in KO mouse lungs are not activated in the neonatal period; nevertheless, ILC2 development is not impaired by IL-33 deficiency as the number of lung ILC2s in adult KO mice did not significantly differ from those in WT mice. However, I.N administration of recombinant IL-33 induced less production of type 2 cytokines, less mucus production and eosinophil infiltration in KO than WT mice. Moreover, lung ILC2s in adult KO mice that received I.N administration of recombinant IL-33 in the neonatal period were no less responsive to IL-33 than WT mouse ILC2s with or without neonatal IL-33 treatment. These results showed that the activation of lung ILC2s by endogenous IL-33 in the neonatal period has significant effects on the functions of lung ILC2s in adulthood.

We have previously shown that adult mouse lung ILC2s activated by I.N administration of allergens or recombinant IL-33 persist for many months as memory ILC2s, which are more responsive to allergen/IL-33 challenges than naive ILC2s (15). Although neonatal lung ILC2 activation appears to have similar effects as the generation of memory ILC2s, there are important differences between the two. Memory ILC2s in adult mice maintain the expression of the IL-25R for many months and acquire the ability to respond to IL-25. Neonatal ILC2s also express the IL-25R and are responsive to IL-25, however, they do not maintain the expression of the IL-25R into adulthood and become unresponsive to IL-25. Therefore, ILC2s do not acquire new

functions by exposure to endogenous neonatal IL-33. Instead, they become more fit in their responses to IL-33, hence the term “training”.

It is unknown why the activation of lung ILC2s by endogenous IL-33 in the neonatal period results in IL-25R^{-} “trained” ILC2s, but not IL-25R^{+} memory ILC2s similar to those generated in adult mice by I.N administration of recombinant IL-33. It is likely that neonatal ILC2 activation is weak as demonstrated by the lack of mucus hyperproduction (data not shown). Based on the gene expression data in the current study, the neonatal activation is weak as neonatal ILC2s do not upregulate some genes including *Il1r2*, *Tnfrsf8*, *Anxa2*, *Pdcd1*, *Ctla4, Nmur1* to the same extent as IL-33 treated adult effector ILC2s. This may be due to the difference in the amount of bioactive IL-33 in the lung. In neonatal lungs, we detected approximately 250 pg/mg of IL-33 whereas in adult lungs given I.N recombinant IL-33, we measured around 150 pg/mg IL-33 (29). However, in contrast to recombinant IL-33, it is difficult to determine how much neonatal IL-33 is nuclear versus cytoplasmic or extracellular and whether it is bioactive and available to stimulate ILC2s (30). It should also be noted that IL-33 alone is not sufficient to activate purified ILC2s in vitro (16) and other stimuli are required including TSLP, IL-7, IL-2, neuropeptides (NMU, CGRP, VIP), or prostaglandins (PGD2) (31). Whether neonatal and adult lungs differ in the amount of these costimulatory molecules remains to be elucidated.

The concept of neonatal ILC2 training implies that naive adult lung ILC2s in WT mice are trained. Untrained ILC2s in IL-33 KO and trained ILC2s in WT mice have a small number of differentially expressed genes. For example, *Hdac3* is downregulated in KO ILC2s. Interestingly, the HDAC inhibitor, trichostatin A, which targets Class I HDACs such as HDAC3

has been shown to downregulate the number of ILC2s expressing IL-5 and IL-13 upon *Alternaria alternata* extract challenge suggesting an important role of HDACs in activation (32). Additionally, WT ILC2s express more *Tnfsf10,* a pro-apoptotic gene, consistent with a cytoprotective function that occurs upon lymphocyte activation (33). DUSP10 encoded by the *Dusp10* gene is normally expressed at low levels in ILC2s. Forced expression of DUSP10 in ILC2s has been shown to inhibit IL-5 and IL-13 production upon IL-33 treatment, attenuating allergic responses (27). The differential expression of *Icos* may imply differences in cell-to-cell contact that may be important for activation of ILC2s. While ICOS:ICOSL interactions between ILC2s have been found to be important for function and survival (34), it also has been shown to inhibit ILC2 responses via interactions with Tregs (35). Additionally, CD24, which regulates cell surface receptor signaling (36), is expressed more on KO ILC2s than WT ILC2s. *Tnf* is a pro-inflammatory associated gene, and it has recently been found to be increased in peripheral tissue ILC2s at steady-state compared to bone marrow ILC2s (37). It remains to be determined whether, in addition to these ILC2 intrinsic differences, there might be differences in lung microenvironments between WT and KO mouse lungs that contribute to ILC2 activation in adulthood.

The term “trained immunity” has been used to describe the phenomenon of memory-like myeloid cells (38). Activation of macrophages by pathogen-derived molecules including β-glucan results in their differentiation into highly functional macrophages that live up to 4 weeks and mediate antigen-nonspecific innate protection against subsequent infections. Naïve macrophages are also trained by helminth infection and acquire the ability to kill larvae in a later infection. Trained immunity in myeloid cells has been shown to be mediated by epigenetic

modifications. It remains to be determined whether similar mechanisms are involved in neonatal ILC2 training.

The neonatal period is critical for the development of lung immunity and establishing the ILC2 population within the lung which plays a critical role in allergic lung diseases. Modulating ILC2 training during childhood could dampen the propensity of ILC2s to develop into effective mediators of allergic disease.

Methods

Mice

C57Bl/6 (B6) were purchased from the Jackson Laboratory and bred and maintained in the British Columbia Cancer Research Centre (BCCRC) animal facility. An equal number of males and females were used for each experiment. B6.*Il33*$^{-/-}$ (obtained from the Knockout Mouse Project Repository) were used and maintained at the BCCRC. Mice were used at 10 days after birth for neonatal experiments and at 4-8 weeks of age for adults.

Primary leukocyte preparation

Cell suspensions were prepared from the lungs as described (39). The protocols were modified for neonatal lungs, which used 2.5 ml of the appropriate digestion buffer for each lung. Single cells from all tissues were counted using a hemocytometer, incubated with 2.4G2 monoclonal antibody (mAb) to block Fc receptors, and stained with fluorochrome-conjugated antibodies (Table 1) and phenotypically analyzed by flow cytometry.

Antibodies and flow cytometry

Antibodies used are listed in Table 1. BD Fortessa was used for phenotypic analysis. FlowJo (Tree Star, Ashland, Oregon) version 8.6 and version 10, were used for data analysis. Lung mouse cells were first gated as Singlets, Live, $CD45^+$ lymphocytes and ILC2s were identified as Lineage (Gr-1, Ter119, CD11b, CD11c, CD19, NK1.1, CD3ε, CD4, TCRβ, TCRγδ)$^-$, $Thy1.2^+$, $CD127^+$, $CD25^+$, $ST2^+$ (Supplemental Figure 1A). Lung mouse eosinophils were identified as Lymph (CD3e, NK1.1, CD19)$^-$, 7/4$^-$. CD11c$^-$, $SiglecF^+$. Total cell numbers were calculated based on their frequency out of Live, $CD45^+$ cells determined by FlowJo multiplied by the hemocytometer total cell count.

Bronchoalveolar lavage (BAL)

Mice were euthanized and a catheter attached to a syringe was inserted into the trachea. 1 ml plain PBS was instilled into the lungs and then collected. The BAL was centrifuged at 400 RCF for 10 minutes and the supernatant was collected. IL-5 and IL-13 were quantified by ELISA (Thermo Fisher Scientific, Waltham, MA) according to manufacturer's protocol.

In vivo stimulation

Intranasal (I.N) injections were given after mice were anesthetized by isoflurane inhalation. The concentration of proteins used intranasally is shown in Table 2.

Intracellular staining

All intracellular staining for IL-5 and IL-13 was performed with the Cytofix/Cytoperm kit (BD Biosciences) after a 3-hour incubation of cells in 500 µl Dulbecco modified Eagle medium

containing 10% FBS, penicillin + streptomycin (P/S), 2-mercaptoethanol (2-ME), Brefeldin A (GolgiPlug, BD Biosciences), PMA (30 ng/ml), and ionomycin (500 ng/ml) (MilliporeSigma) at 37°C. Dead cells were excluded with eFluor780 (Thermo Fisher Scientific) fixable viability dye. Ki-67 staining was performed without incubation using the Foxp3/Transcription Factor Staining Buffer Set (Thermo Fisher Scientific) according to the manufacturer's protocol.

5-bromo-2'-deoxyuridine (BrdU)

Neonates were given 0.8 mg of BrdU (MilliporeSigma) in 10 µl preheated PBS for four days starting at day 6-9 after birth. Adult mice were given BrdU at the concentration of 0.8 mg/ml in sterilized drinking water. To ensure that mice drank the water, 20% dextrose was added. Light sensitive bottles were used to protect BrdU. Water was changed every two days. One mouse was euthanized per week to check the incorporation of BrdU. After harvesting the lungs from BrdU treated adults or neonates, single-cell suspensions were prepared from lung tissues and cells were stained with viability dye and antibodies for surface markers to identify ILC2s. Cells were then fixed, followed by staining of BrdU using the APC BrdU Flow Kit (BD Biosciences). For BrdU and IL-13 staining, cells were first incubated with PMA, ionomycin and GolgiPlug for 3 hours at 37°C. After, the cells were harvested and fixed using the APC BrdU Flow Kit and then stained for both IL-13 and BrdU.

ILC2 enrichment and sorting

Individual mouse lungs were prepared as described previously and after lysing, were pooled, and the suspension was then enriched for ILC2s using EasySep Mouse ILC2 Enrichment Kit

(STEMCELL Technologies) according to manufacturer's protocol. BD Aria was used for purity sort of ILC2s identified as Lineage$^-$, Thy1.2$^+$, ST2$^+$, CD127$^+$ (Supplemental Figure 1B).

Microarray

Total RNA was isolated using TRIzol (Life Technologies). RNA was quantified and checked for quality by Agilent Bioanalyzer 2100. RNA amplification, and microarray services were performed by the Centre for Applied Genomics, Toronto, Ontario, using the Affymetrix GeneChip Mouse Gene 2.0ST Array. The expression profile was normalized using robust multi-array (RMA) algorithm. All data analysis was performed with FlexArray 1.6 (Genome Quebec). The microarray data discussed in this publication have been deposited in NCBI's Gene Expression Omnibus and are accessible through GEO Series accession number GSE148539 for Figure 1G and GSE148545 for Figure 4A.
(https://www.ncbi.nlm.nih.gov/geo/query/acc.cgi?acc=GSE148539,
https://www.ncbi.nlm.nih.gov/geo/query/acc.cgi?acc=GSE148545).

Gene Set Enrichment Analysis (GSEA)

GSEA was performed using GSEA software. Log2-fold expression values for each comparison were ranked in descending order and then run through GSEA V2.2.2 available from http://software.broadinstitute.org/gsea/index.jsp (40). The gene set collections that were used were C7 immunologic signatures (41), with the following parameters: number of permutations: 1000; number of genes plotted per graph: 200. High normalized enrichment scores and low false discovery rates indicated that the similarity between a priori gene set and the two states analyzed was highly significant.

cDNA synthesis

cDNA was prepared from 1.5 µg RNA using high-capacity cDNA reverse transcription kit (Thermo Fisher Scientific) according to manufacturer's protocol.

RT-qPCR

RT-qPCR was carried out by StepOnePlus system (Thermo Fisher Scientific) using TaqMan fast reagents. 75 ng of cDNA was used per reaction and the following probe/primers sets were used for detection: *Il1r2* (IDT Assay ID – Mm.PT.58.30874994): Probe -5'-/56-FAM/CCCATTACA/ZEN/TCGGAGAAGCCCACA/3IABkFQ/-3', Primer 1 – 5'TGCTTTCACCACTCCAACAG-3', Primer 2 – 5'CCTTCCAGCCTCAATTCAGAT-3'; *Nmur1* (IDT Assay ID – Mm.PT.58.32232111), Probe – 5'-/56-FAM/ACCACAACC/ZEN/AGTGCAAACAGCATC/3IABkFQ/-3', Primer 1 -5'-AGGATTCAGCTGCAAGATAGG-3', Primer 2 – 5'-ATACGGTCAGCATGGAATGG-3'; *Vegfa* (IDT Assay ID – Mm.PT.58.14200306), Probe - 5'-/56-FAM/TGCTGTACC/ZEN/TCCACCATGCCAAG/3IABkFQ/-3', Primer 1 -5'-CCGAAACCATGAACTTTCTGC-3', Primer 2 – 5'-GACTTCTGCTCTCCTTCTGTC-3'; Tbp (IDT Assay ID – Mm.PT.39a.22214839), Probe – 5'-/56-FAM/ACTTGACCT/ZEN/AAAGACCATTGCACTTCGT/3IABkFQ/-3', Primer 1 – 5'-TGTATCTACCGTGAATCTTGGC-3', Primer 2 – 5'-CCAGAACTGAAAATCAACGCAG-3'. Acquired data were analyzed by the 2-ΔΔCt method (42). Threshold cycles were normalized to the expression of Tbp and then to adult naïve ILC2s (controls).

Lung homogenate preparation and analyses

Lungs were collected from naive mice at various days after birth and homogenized in HBSS with EDTA and Halt protease inhibitor cocktail (Thermo Fisher Scientific) at 200 mg per lung tissue per ml. After centrifugation at 800 RCF for 20 min, supernatant was analyzed using IL-33 ELISA (Thermo Fisher Scientific) according to manufacturer's protocols. Total protein was quantified using the Protein Quantification Kit-Rapid (MilliporeSigma). The amount of IL-33 per sample (pg) was normalized by the total amount of protein within the lung homogenate (mg).

Periodic acid-Schiff (PAS) staining

Lungs were perfused with 1 ml (adults) 4% paraformaldehyde and harvested. Fixed lungs were embedded in paraffin by the Centre for Translational and Applied Genomics (Vancouver, Canada), and 4-μm sections placed on glass. Slides were Periodic-Acid Schiff (PAS)-stained by the Department of Pathology at Vancouver General Hospital (Vancouver, Canada). To quantify the PAS positive area, ImageJ was used as previously described (with a magnification of 4x) (43, 44). Results were expressed as PAS-positive area (square millimeters) per mm of basement membrane length.

Statistics

Data were analyzed with GraphPad Prism 6 (GraphPad Software, La Jolla, Calif). Unpaired Student's 1-tailed *t* test was used to determine statistical significance between groups or for multiple comparisons 2-way (Figure 1D, 1E) and 1-way (Figure 5G-I) ANOVA with Bonferroni post hoc test. n refers to an individual biological replicate unless otherwise specified. Data in plots represent the mean ± SEM. A P value less than 0.05 was considered significant. (*P < .05, **P < .01, ***P < .005, ****P < .0001, NS, not significantly different [P > .05]).

Study approval

All animal use was approved by the animal care committee of the University of British Columbia in accordance with the guidelines of the Canadian Council on Animal Care. Genotyping was done by the Biomedical Research Centre Genotyping Facility.

Author contributions

C.A.S designed and performed experiments and wrote the manuscript. L.M and H.S performed experiments. F.T designed experiments and wrote the manuscript.

Acknowledgments

C.A.S is the recipient of a UBC Four Year Fellowship and a CIHR studentship. L.M. is a recipient of a UBC Four Year Fellowship and a Vanier Canada Graduate Scholarship. This work was supported by grants from the Canadian Institute of Health Research (PJT-153304, MOP-126194).

References:

1. Martinez-Gonzalez I, Steer CA, Takei F. Lung ILC2s link innate and adaptive responses in allergic inflammation. *Trends in immunology*. Mar 2015;36(3):189-95. doi:10.1016/j.it.2015.01.005
2. Gieseck RL, 3rd, Wilson MS, Wynn TA. Type 2 immunity in tissue repair and fibrosis. *Nature reviews Immunology*. Jan 2018;18(1):62-76. doi:10.1038/nri.2017.90
3. Halim TY, Steer CA, Matha L, et al. Group 2 innate lymphoid cells are critical for the initiation of adaptive T helper 2 cell-mediated allergic lung inflammation. *Immunity*. Mar 20 2014;40(3):425-35. doi:10.1016/j.immuni.2014.01.011
4. Oliphant CJ, Hwang YY, Walker JA, et al. MHCII-mediated dialog between group 2 innate lymphoid cells and CD4(+) T cells potentiates type 2 immunity and promotes parasitic helminth expulsion. *Immunity*. Aug 21 2014;41(2):283-95. doi:10.1016/j.immuni.2014.06.016
5. Halim TYF, Rana BMJ, Walker JA, et al. Tissue-Restricted Adaptive Type 2 Immunity Is Orchestrated by Expression of the Costimulatory Molecule OX40L on Group 2 Innate Lymphoid Cells. *Immunity*. Jun 19 2018;48(6):1195-1207 e6. doi:10.1016/j.immuni.2018.05.003
6. Halim TY, Hwang YY, Scanlon ST, et al. Group 2 innate lymphoid cells license dendritic cells to potentiate memory TH2 cell responses. *Nature immunology*. Jan 2016;17(1):57-64. doi:10.1038/ni.3294
7. Dahlgren MW, Molofsky AB. All along the watchtower: group 2 innate lymphoid cells in allergic responses. *Curr Opin Immunol*. Oct 2018;54:13-19. doi:10.1016/j.coi.2018.05.008
8. Schuijs MJ, Halim TYF. Group 2 innate lymphocytes at the interface between innate and adaptive immunity. *Annals of the New York Academy of Sciences*. Apr 2018;1417(1):87-103. doi:10.1111/nyas.13604
9. Gasteiger G, Fan X, Dikiy S, Lee SY, Rudensky AY. Tissue residency of innate lymphoid cells in lymphoid and nonlymphoid organs. *Science*. Nov 20 2015;350(6263):981-5. doi:10.1126/science.aac9593
10. Schneider C, Lee J, Koga S, et al. Tissue-Resident Group 2 Innate Lymphoid Cells Differentiate by Layered Ontogeny and In Situ Perinatal Priming. *Immunity*. Jun 18 2019;50(6):1425-1438 e5. doi:10.1016/j.immuni.2019.04.019
11. Steer CA, Martinez-Gonzalez I, Ghaedi M, Allinger P, Matha L, Takei F. Group 2 innate lymphoid cell activation in the neonatal lung drives type 2 immunity and allergen sensitization. *The Journal of allergy and clinical immunology*. Aug 2017;140(2):593-595 e3. doi:10.1016/j.jaci.2016.12.984
12. de Kleer IM, Kool M, de Bruijn MJ, et al. Perinatal Activation of the Interleukin-33 Pathway Promotes Type 2 Immunity in the Developing Lung. *Immunity*. Dec 20 2016;45(6):1285-1298. doi:10.1016/j.immuni.2016.10.031
13. Saluzzo S, Gorki AD, Rana BMJ, et al. First-Breath-Induced Type 2 Pathways Shape the Lung Immune Environment. *Cell reports*. Feb 21 2017;18(8):1893-1905. doi:10.1016/j.celrep.2017.01.071
14. Dahlgren MW, Jones SW, Cautivo KM, et al. Adventitial Stromal Cells Define Group 2 Innate Lymphoid Cell Tissue Niches. *Immunity*. Mar 19 2019;50(3):707-722 e6. doi:10.1016/j.immuni.2019.02.002

15. Martinez-Gonzalez I, Matha L, Steer CA, Ghaedi M, Poon GF, Takei F. Allergen-Experienced Group 2 Innate Lymphoid Cells Acquire Memory-like Properties and Enhance Allergic Lung Inflammation. *Immunity*. Jul 19 2016;45(1):198-208. doi:10.1016/j.immuni.2016.06.017
16. Halim TY, Krauss RH, Sun AC, Takei F. Lung natural helper cells are a critical source of Th2 cell-type cytokines in protease allergen-induced airway inflammation. *Immunity*. Mar 23 2012;36(3):451-63. doi:10.1016/j.immuni.2011.12.020
17. Lang D, Knop J, Wesche H, et al. The type II IL-1 receptor interacts with the IL-1 receptor accessory protein: a novel mechanism of regulation of IL-1 responsiveness. *Journal of immunology*. Dec 15 1998;161(12):6871-7.
18. Knolle MD, Chin SB, Rana BMJ, et al. MicroRNA-155 Protects Group 2 Innate Lymphoid Cells From Apoptosis to Promote Type-2 Immunity. *Frontiers in immunology*. 2018;9:2232. doi:10.3389/fimmu.2018.02232
19. Johansson K, Malmhall C, Ramos-Ramirez P, Radinger M. MicroRNA-155 is a critical regulator of type 2 innate lymphoid cells and IL-33 signaling in experimental models of allergic airway inflammation. *The Journal of allergy and clinical immunology*. Mar 2017;139(3):1007-1016 e9. doi:10.1016/j.jaci.2016.06.035
20. Heshmat NM, El-Hadidi ES. Soluble CD30 serum levels in atopic dermatitis and bronchial asthma and its relationship with disease severity in pediatric age. *Pediatric allergy and immunology : official publication of the European Society of Pediatric Allergy and Immunology*. Jun 2006;17(4):297-303. doi:10.1111/j.1399-3038.2006.00405.x
21. Katsunuma T, Kawahara H, Suda T, et al. Analysis of gene expressions of T cells from children with acute exacerbations of asthma. *International archives of allergy and immunology*. May 2004;134(1):29-33. doi:10.1159/000077530
22. Sekigawa T, Tajima A, Hasegawa T, et al. Gene-expression profiles in human nasal polyp tissues and identification of genetic susceptibility in aspirin-intolerant asthma. *Clinical and experimental allergy : journal of the British Society for Allergy and Clinical Immunology*. Jul 2009;39(7):972-81. doi:10.1111/j.1365-2222.2009.03229.x
23. Schwartz C, Khan AR, Floudas A, et al. ILC2s regulate adaptive Th2 cell functions via PD-L1 checkpoint control. *The Journal of experimental medicine*. Sep 4 2017;214(9):2507-2521. doi:10.1084/jem.20170051
24. Salimi M, Wang R, Yao X, et al. Activated innate lymphoid cell populations accumulate in human tumour tissues. *BMC cancer*. Mar 27 2018;18(1):341. doi:10.1186/s12885-018-4262-4
25. Wallrapp A, Riesenfeld SJ, Burkett PR, et al. The neuropeptide NMU amplifies ILC2-driven allergic lung inflammation. *Nature*. Sep 21 2017;549(7672):351-356. doi:10.1038/nature24029
26. Ghaedi M, Steer CA, Martinez-Gonzalez I, Halim TY, Abraham N, Takei F. Common-Lymphoid-Progenitor-Independent Pathways of Innate and T Lymphocyte Development. *Cell reports*. Apr 19 2016;15(3):471-80. doi:10.1016/j.celrep.2016.03.039
27. Yamamoto T, Endo Y, Onodera A, et al. DUSP10 constrains innate IL-33-mediated cytokine production in ST2(hi) memory-type pathogenic Th2 cells. *Nature communications*. Oct 12 2018;9(1):4231. doi:10.1038/s41467-018-06468-8
28. Zhao J, Wei J, Bowser RK, Traister RS, Fan MH, Zhao Y. Focal adhesion kinase-mediated activation of glycogen synthase kinase 3beta regulates IL-33 receptor internalization and IL-

33 signaling. *Journal of immunology*. Jan 15 2015;194(2):795-802. doi:10.4049/jimmunol.1401414
29. Matha L, Shim H, Steer CA, Yin YH, Martinez-Gonzalez I, Takei F. Female and male mouse lung group 2 innate lymphoid cells differ in gene expression profiles and cytokine production. *PloS one*. 2019;14(3):e0214286. doi:10.1371/journal.pone.0214286
30. Cayrol C, Girard JP. Interleukin-33 (IL-33): A nuclear cytokine from the IL-1 family. *Immunological reviews*. Jan 2018;281(1):154-168. doi:10.1111/imr.12619
31. Hurrell BP, Shafiei Jahani P, Akbari O. Social Networking of Group Two Innate Lymphoid Cells in Allergy and Asthma. *Frontiers in immunology*. 2018;9:2694. doi:10.3389/fimmu.2018.02694
32. Toki S, Goleniewska K, Reiss S, et al. The histone deacetylase inhibitor trichostatin A suppresses murine innate allergic inflammation by blocking group 2 innate lymphoid cell (ILC2) activation. *Thorax*. Jul 2016;71(7):633-45. doi:10.1136/thoraxjnl-2015-207728
33. Falschlehner C, Ganten TM, Koschny R, Schaefer U, Walczak H. TRAIL and other TRAIL receptor agonists as novel cancer therapeutics. *Advances in experimental medicine and biology*. 2009;647:195-206. doi:10.1007/978-0-387-89520-8_14
34. Maazi H, Patel N, Sankaranarayanan I, et al. ICOS:ICOS-ligand interaction is required for type 2 innate lymphoid cell function, homeostasis, and induction of airway hyperreactivity. *Immunity*. Mar 17 2015;42(3):538-51. doi:10.1016/j.immuni.2015.02.007
35. Rigas D, Lewis G, Aron JL, et al. Type 2 innate lymphoid cell suppression by regulatory T cells attenuates airway hyperreactivity and requires inducible T-cell costimulator-inducible T-cell costimulator ligand interaction. *The Journal of allergy and clinical immunology*. May 2017;139(5):1468-1477 e2. doi:10.1016/j.jaci.2016.08.034
36. Ayre DC, Christian SL. CD24: A Rheostat That Modulates Cell Surface Receptor Signaling of Diverse Receptors. *Frontiers in cell and developmental biology*. 2016;4:146. doi:10.3389/fcell.2016.00146
37. Ricardo-Gonzalez RR, Van Dyken SJ, Schneider C, et al. Tissue signals imprint ILC2 identity with anticipatory function. *Nature immunology*. Oct 2018;19(10):1093-1099. doi:10.1038/s41590-018-0201-4
38. Netea MG, van der Meer JW. Trained Immunity: An Ancient Way of Remembering. *Cell host & microbe*. Mar 8 2017;21(3):297-300. doi:10.1016/j.chom.2017.02.003
39. Romera-Hernandez M, Matha L, Steer CA, Ghaedi M, Takei F. Identification of Group 2 Innate Lymphoid Cells in Mouse Lung, Liver, Small Intestine, Bone Marrow, and Mediastinal and Mesenteric Lymph Nodes. *Current protocols in immunology / edited by John E Coligan [et al]*. Apr 17 2019:e73. doi:10.1002/cpim.73
40. Subramanian A, Tamayo P, Mootha VK, et al. Gene set enrichment analysis: a knowledge-based approach for interpreting genome-wide expression profiles. *Proceedings of the National Academy of Sciences of the United States of America*. Oct 25 2005;102(43):15545-50. doi:10.1073/pnas.0506580102
41. Godec J, Tan Y, Liberzon A, et al. Compendium of Immune Signatures Identifies Conserved and Species-Specific Biology in Response to Inflammation. *Immunity*. Jan 19 2016;44(1):194-206. doi:10.1016/j.immuni.2015.12.006
42. Livak KJ, Schmittgen TD. Analysis of relative gene expression data using real-time quantitative PCR and the 2(-Delta Delta C(T)) Method. *Methods*. Dec 2001;25(4):402-8. doi:10.1006/meth.2001.1262

43. Zuberi RI, Ge XN, Jiang S, et al. Deficiency of endothelial heparan sulfates attenuates allergic airway inflammation. *Journal of immunology*. Sep 15 2009;183(6):3971-9. doi:10.4049/jimmunol.0901604
44. Ge XN, Bahaie NS, Kang BN, et al. Allergen-induced airway remodeling is impaired in galectin-3-deficient mice. *Journal of immunology*. Jul 15 2010;185(2):1205-14. doi:10.4049/jimmunol.1000039

Figure 1:

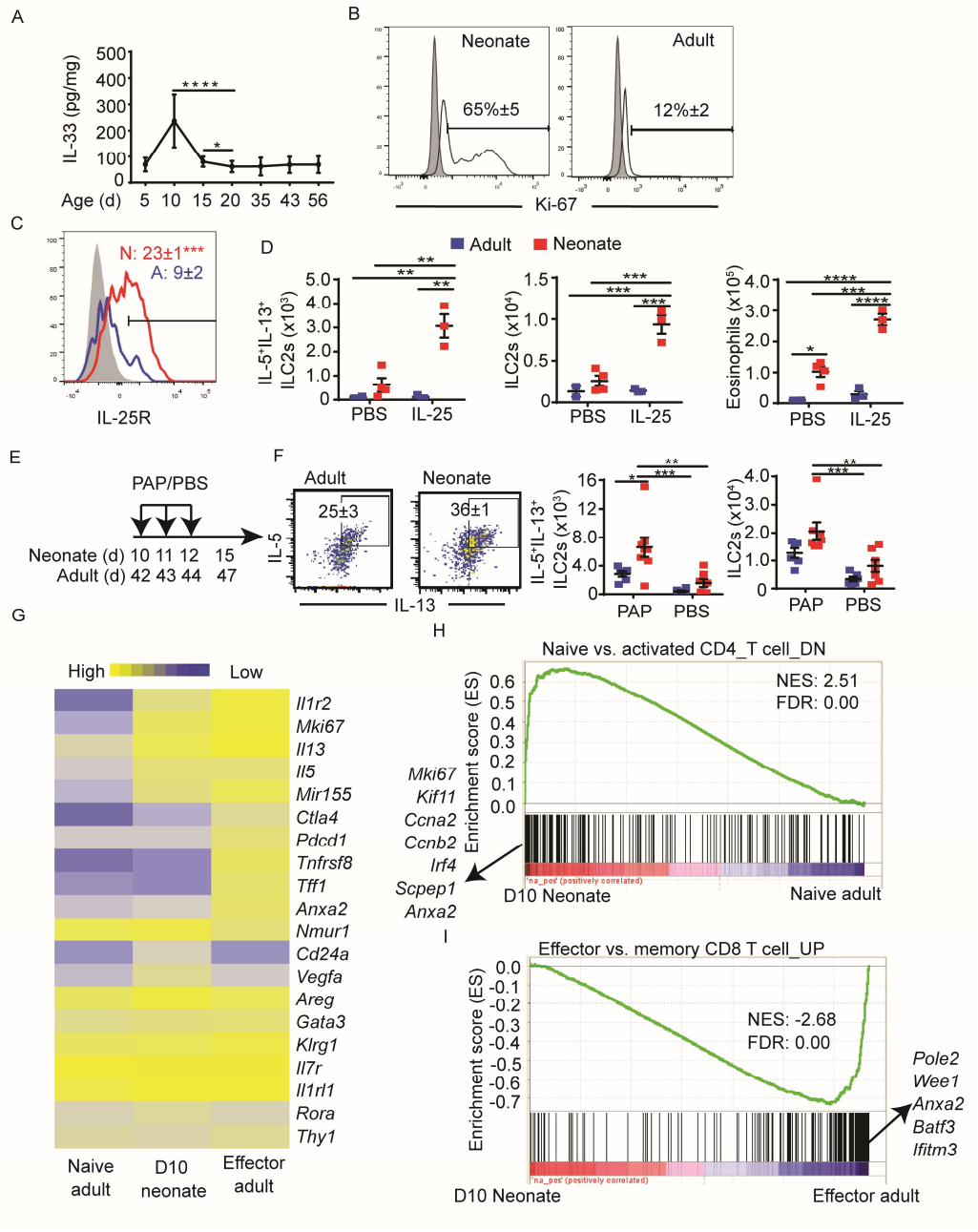

Figure 1: Neonatal ILC2s are activated by endogenous IL-33.

(A) The amount of IL-33 in whole lung homogenates of naïve mice at indicated ages (n>4). (B) Ki-67 expression of neonatal (d10) and adult (4-6 weeks) lung ILC2s (gated as in Supplemental Figure 1A) (n=4). Shaded = isotype control. Open = anti-Ki-67. (C) Neonatal and adult ILC2s

were examined for IL-25R/IL-17RB expression (n=5). Shaded = isotype control. Numbers in plot indicate the mean percentage ± SEM. (D) B6 neonates (red squares) and adults (blue squares) were treated with one administration of I.N IL-25 on postnatal day 10 and 42 respectively. 3 days later, numbers of IL-5^{+}IL-13^{+} ILC2s (left), total ILC2s (centre), and eosinophils (right) in the lungs were analyzed by flow cytometry (n=3-4, 2 independent experiments). (E) Scheme of I.N papain (PAP)/PBS injections (n=5-8, 2 independent experiments). (d)=Days after birth. (F) Flow cytometry plots show intracellular IL-5 and IL-13 expression in ILC2s in adult and neonatal papain-treated mice. Numbers in flow plots are percentage of double positive ILC2s ± SEM. Scatter plots show numbers of IL-5^{+}IL-13^{+} ILC2s (left) and total ILC2s (right). Blue squares=Adults; Red squares=Neonates. (G) Heatmap shows the relative expression levels of genes in lung ILC2s from naïve adults (8 weeks of age), day 10 neonatal pups and effector adults (8 weeks of age) that have been given three 0.25 μg IL-33 I.N injections and then harvested one day after the last injection (n=3 per condition, each replicate represents sorted ILC2s from 8 pooled mice). (H) Gene set enrichment analysis (GSEA) of neonatal ILC2s vs naïve adult ILC2s. The Log2-fold change for each comparison was ranked in descending order and compared to the immunological signatures gene set (C7). The x axis shows where the members of the gene set appear in the ranked list of genes. The y axis is the enrichment score. The highest ranked genes are listed on the x axis of each panel. The genes that were downregulated in naïve CD4 T cells compared to activated CD4 T cells were significantly enriched in neonatal day 10 ILC2s. (I) GSEA of neonatal ILC2s and effector adult ILC2s. Genes that were upregulated in effector CD8 T cells compared to memory CD8 T cells were enriched in effector adult ILC2s. NES; Normalized Enrichment score; FDR; false discovery rate. *P < .05.

**P < .01. ***P < .005 (1-tailed unpaired Student's *t* test for Figure 1C, 2-way ANOVA with Bonferroni post hoc test for Figure 1D, F).

Figure 2:

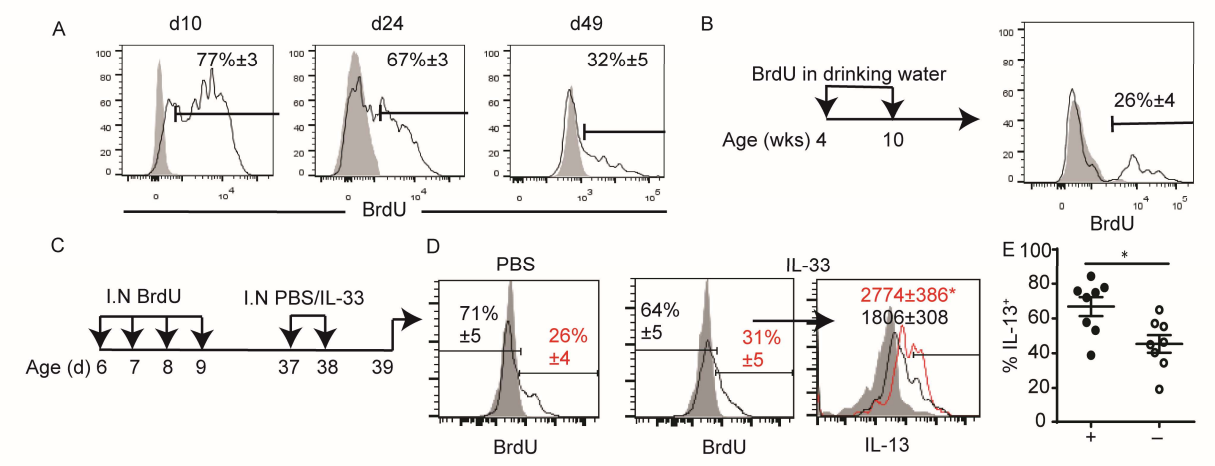

Figure 2: ILC2s labelled with BrdU in the neonatal period respond more intensely than BrdU$^-$ ILC2s to IL-33 treatment later in life.

(A) BrdU was administered I.N at postnatal day (d) 6-9. Lung ILC2s were analyzed at indicated ages for BrdU (n>4). Shaded = isotype control. Open = anti-BrdU. (B) Adult mice were given BrdU in their drinking water for 6 weeks as indicated by the scheme and analyzed for ILC2 incorporation of BrdU (histogram). Numbers in plots represent mean % ± SEM (n=9, 2 independent experiments). (C) Mice received BrdU and IL-33 I.N administrations as shown. (D) Lung ILC2s in PBS injected (left histogram) and IL-33 injected (middle) mice were stained by anti-BrdU (open) or isotype control (shaded). Numbers in plots represent mean % ± SEM. Right histograms show intracellular IL-13 in BrdU$^+$ (red line) and BrdU$^-$ (black line) ILC2s from IL-33 injected mice with isotype control (shaded). Numbers in plot show mean fluorescence intensity ± SEM. (E) Scatter plot shows the percentages of IL-13$^+$ cells among BrdU$^+$ (black) and BrdU$^-$ (open) ILC2s (n=8, 2 independent experiments). *P < .05 (1-tailed unpaired Student's *t* test).

Figure 3:

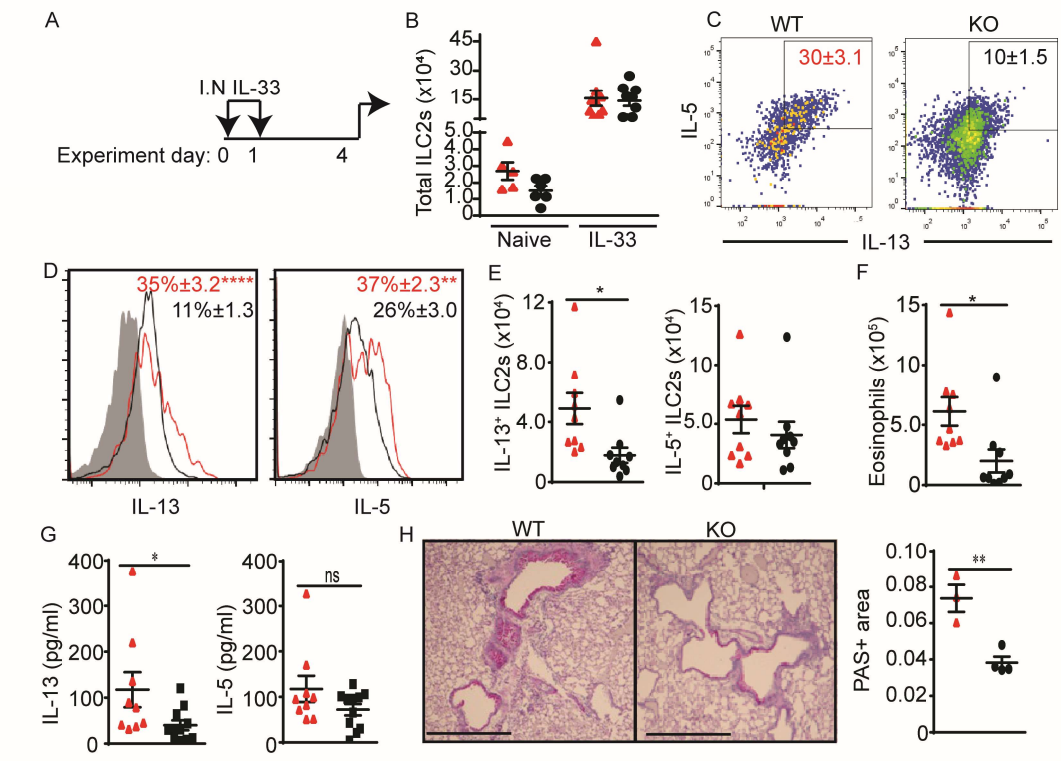

Figure 3: ILC2s from IL-33 deficient mice respond more weakly than WT mice to IL-33 treatment.

(A) Adult WT (red) and KO (black) mice at 8 weeks of age received two daily I.N IL-33 administrations and were analyzed three days later (n=9, 3 independent experiments). (B) Total number of lung ILC2s in naive and IL-33 treated WT and KO mice. (C) Plots show intracellular IL-5 and IL-13 expression in WT and KO ILC2s. Numbers in plots represent mean % ± SEM. (D) Histograms of intracellular IL-13 (left) and IL-5 (right) staining in WT and KO ILC2s. Numbers in plots represent mean percentage ± SEM. Shaded=isotype control. (E) Numbers of IL-13$^+$ (left scatter plot) and IL-5$^+$ (right scatter plot) ILC2s. (F) Eosinophil numbers in the lung. (G) The amount of IL-13 (left) and IL-5 (right) in the bronchoalveolar lavage. (H) Mucus production by PAS staining of lung tissue sections (left) and PAS+ area (mm^2 per mm of

basement membrane) (right bar graph) (n=4). Scale bar = 0.05mm *P < .05, **P < .01, ****P < .0001 (1-tailed unpaired Student's *t* test).

Figure 4:

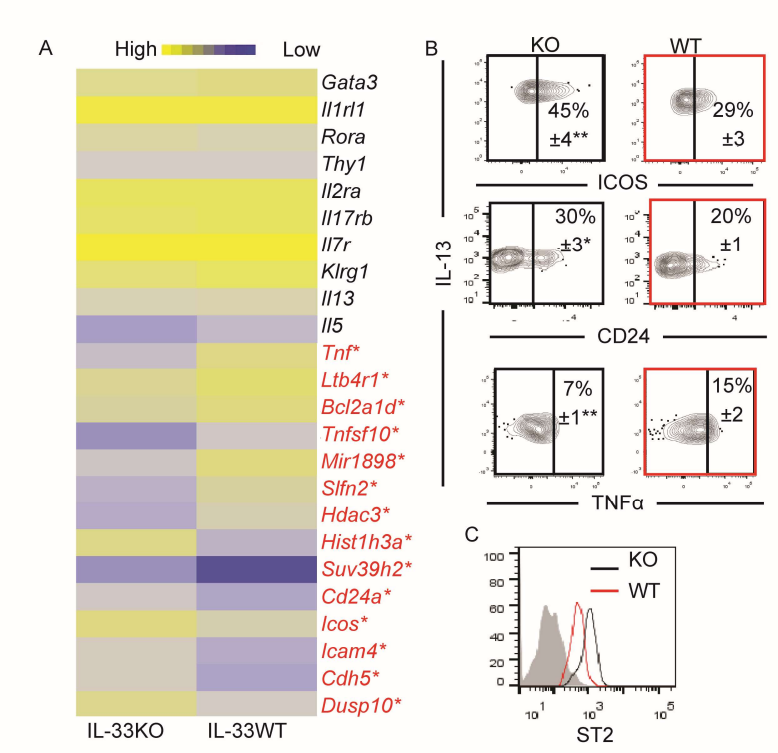

Figure 4: Comparison of IL-33-deficeint (KO) and wildtype (WT) adult ILC2s.

(A) Heatmap shows the relative expression levels of genes that are differentially expressed in lung ILC2s from adult KO (n=2) and WT mice (n=3). Each replicate represents sorted ILC2s from 8 pooled mice *genes in red indicate those that are differentially expressed more than two-fold between KO and WT ILC2s. (B) Flow cytometry plots show expression of CD24, ICOS and intracellular TNF on KO (black) and WT (red) adult mouse lung ILC2s (n=6). Numbers in plot indicate the mean percentage ± SEM. (C) Histograms show ST2 expression on KO and WT ILC2s. Shaded=isotype control. *P < .05, **P < .01. (1-tailed unpaired Student's *t* test for Figures 4B, C).

Figure 5:

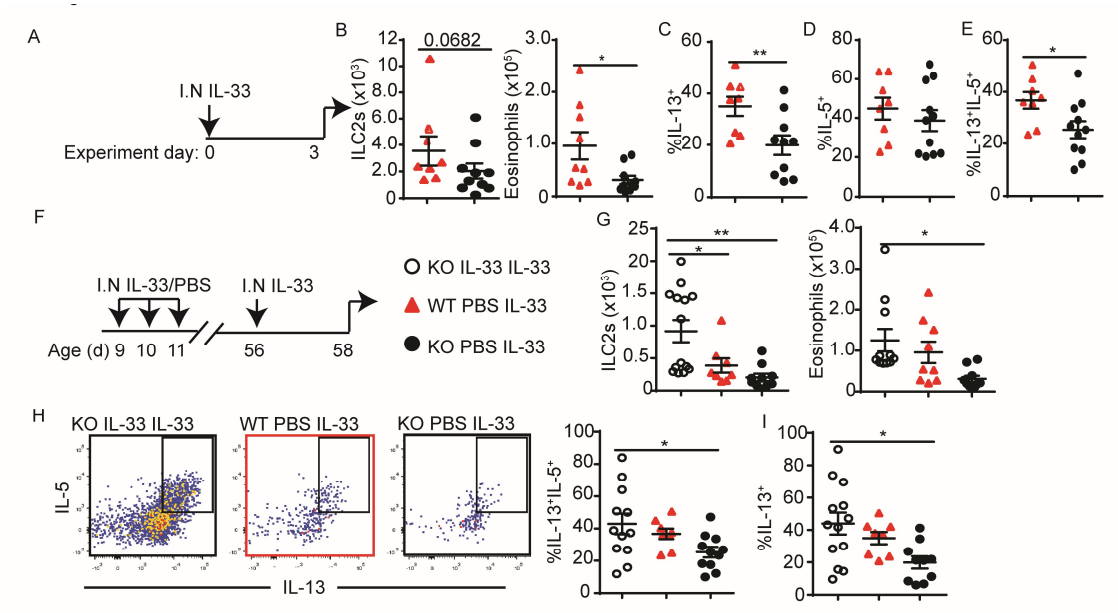

Figure 5: Intranasal IL-33 administration in the neonatal period rescues impaired KO ILC2 responses in adulthood.

(A)WT (n=9) (red triangles) and KO (n=11) (black circles) mice were treated with I.N IL-33 in adulthood. (B) Total numbers of ILC2s and eosinophils. (C) Frequency of IL-13$^+$ and (D) IL-5$^+$ ILC2s. (E) Frequency of IL-5$^+$IL-13$^+$ ILC2s. (F) KO mice (open circles) were treated with three daily I.N IL-33 as neonates and challenged with IL-33 in adulthood (n=13). WT (red triangles) and KO control mice (black circles) did not receive IL-33 as neonates. (G) Total numbers of ILC2s and eosinophils. (H) Flow cytometry plots show intracellular IL-5 and IL-13 expression and bar graph shows frequency of IL-13$^+$IL-5$^+$ ILC2s. (I) Frequency of IL-13$^+$ ILC2s. Data representative of 4 independent experiments. *P < .05, **P < .01. (1-tailed unpaired Student's *t* test for Figure 5B-E, 1-way ANOVA with Bonferroni post hoc test for Figure 5G-I).

Table 1: List of antibodies used for flow cytometry sorting and analysis.

Target	Detects	Conjugated	Clone	Vendor
7/4	Neutrophils	FITC	7/4	Abcam (Cambridge, UK)
CD11b (Mac-1)	Granulocytes	FITC, eFluor 450	M1/70	Thermo Fisher Scientific
CD11c	DC, monocytes, macrophages, neutrophils	eFluor 450, Alexa Fluor 700	N418	Thermo Fisher Scientific
CD127 (IL-7Rα)	Lymphocytes, progenitors	PE, PE/Cy7, Alexa Fluor 700	A7R34	Thermo Fisher Scientific
CD19	B cells	FITC, PerCP-Cy5.5, eFluor 450	1D3	Thermo Fisher Scientific
CD24	Naïve	PE/Cy7	M1/69	Thermo Fisher Scientific
CD25 (IL-2Ra)	ILC2s, Tregs, progenitors	PerCP-Cy5.5	PC61.5	Thermo Fisher Scientific
CD3ε	T cells, NKT	FITC, PerCP-Cy5.5, eFluor 450	145-2C11	Thermo Fisher Scientific
CD4	T cells, NKT	FITC, eFluor 450, PE/Cy7	RM4-5	Thermo Fisher Scientific
CD45.2	$Ly5.2^{+}$ leukocytes	V500	104	BD Biosciences (San Jose, CA)
CTLA4	Activated T cells and ILC2s	APC	UC10-4B9	Thermo Fisher Scientific
DX5 (CD49b)	NK cells, basophils	PE/Cy7	DX5	Thermo Fisher Scientific
FcεR1α	Mast cells, basophils	APC	CRA1	Thermo Fisher Scientific
Gr-1 (Ly-6G/Ly-6C)	Granulocytes	FITC, eFluor 450	RB6-8C5	Thermo Fisher Scientific
IL-13	ILC2s, Th2	PE	eBio13A	Thermo Fisher Scientific
IL-25R (IL-17RB)	Th2, ILC2s, NKT cells	PE	MUNC33	Thermo Fisher Scientific
IL-4	Th2 cells	APC	11B11	Thermo Fisher Scientific
IL-5	ILC2s	APC	TRFK5	BD Biosciences
Ki-67	Cycling cells	FITC	SolA15	Thermo Fisher Scientific
NK1.1	NK cells	FITC, PerCP-Cy5.5, eFluor 450	PK136	Thermo Fisher Scientific

Target	Detects	Conjugated	Clone	Vendor
Rat IgG1, κ isotype	Isotype control for IL-4, IL-13, and IL-5	APC PE	R3-34 eBRG1	Thermo Fisher Scientific
Rat IgG2b, κ isotype	Isotype control for GATA3 and Ki-67	PE FITC	eB149/10H5 eBR2a	Thermo Fisher Scientific
Siglec-F	Eosinophils	PE	E50-2440	BD Biosciences
T1/ST2 (IL-33R)	ILC2s, eosinophils	FITC	DJ8	MD Bioproduct (Oakdale, MN)
TCRβ	TCR β chain	eFluor 450	H57-597	Thermo Fisher Scientific
TCRγδ	γδ T cells	eFluor 450	GL-3	Thermo Fisher Scientific
Ter119	Erythroid cells	FITC, eFluor 450	Ter-119	Thermo Fisher Scientific
Thy1.2 (CD90.2)	ILCs, T cells	Brilliant Violet 605	DJ8	BD Biosciences
TNF alpha	T cells, neutrophils, macrophages	PE	MP6-XT22	Thermo Fisher Scientific

List of the antibody target, the cells that they detect, the fluorophores they are conjugated to, the specific clones, and the manufacturer. eFluor 780 Fixable Viability Dye (Thermo Fisher Scientific) were used to exclude nonviable cells.

Table 2: Concentrations of intranasal administered treatments.

	Vendor	Adult	Neonate
Papain	MilliporeSigma	0.218 U/40 µl	0.0436 U/10 µl
IL-25	BioLegend (San Diego, CA)	1 µg/40 µl	0.2 µg/10 µl
IL-33	Thermo Fisher Scientific or BioLegend	0.5 µg/40 µl	0.1 µg/10 µl

List of I.N treatments specifying vendor and concentration given to either adults or neonates. All stock concentrations were diluted in plain PBS to achieve working concentrations.